A model for partially dependent component damage fragilities in seismic risk analysis

Jack W. Baker, M.EERI[1,2], Ed Almeter, M.EERI[1], Dustin Cook, M.EERI[3], Abbie B. Liel, M.EERI[4], and Curt Haselton, M.EERI[1]

Abstract

This paper proposes a model to quantify dependencies in component damage in the FEMA P-58 seismic performance assessment methodology, and to simulate damage realizations with the desired dependencies. The model is compatible with the prior FEMA P-58 procedure, and can quantify more realistic dependencies in component damage with only minor changes to the calculation algorithm and model parameters. This paper introduces the proposed model and compares it with the prior procedure. Example calculations are then used to illustrate the quantitative impacts of component damage dependencies on building-level performance metrics. The model is relatively simple to conceptualize and parameterize, so that the degree of dependency can be easily estimated and documented. Given the improved conceptual framing of the problem, and the significant changes it sometimes produces in building-level performance predictions, this model represents an improvement to the general FEMA P-58 seismic performance assessment methodology.

[1]Haselton Baker Risk Group, LLC, Chico, CA, USA
[2]Stanford University, Stanford, CA, USA
[3]National Institute of Standards and Technology (NIST), Gaithersburg, MD, USA
[4]University of Colorado, Boulder, CO, USA

Corresponding author:
Jack Baker, Stanford University, 473 Via Ortega, MC 4020, Stanford, CA 94305-4020, USA
Email: bakerjw@stanford.edu

*Prepared using sagej.cls [Version: 2017/01/17 v1.20]*

Introduction

The FEMA (2018) P-58 seismic risk assessment procedure is appealing because it considers structure-specific features and quantifies a range of performance metrics relevant to decision-makers (Haselton et al., 2018). FEMA P-58 builds upon and standardizes prior performance-based and assembly-based loss assessment procedures (Cornell and Krawinkler, 2000; Porter et al., 2001; Moehle and Deierlein, 2004). Given a ground shaking amplitude (which can be specified as a single amplitude or probabilistically), the procedure assesses building response, damage to individual components of the building, and then the costs and recovery time of that damage. The procedure is Monte-Carlo-based, where each stage of analysis is performed by sampling realizations from specified probability distributions, and the set of simulated results is used to quantify the distribution of predicted consequences.

This paper is concerned with the component damage stage of the FEMA P-58 analysis. Component damage is simulated by utilizing an Engineering Demand Parameter (EDP), such as a displacement or acceleration at a given location in the building, and a fragility function to compute the resulting probability of a component experiencing a given damage state.

Dependencies in the damage states of individual building components are an important consideration in building damage, but the prior FEMA P-58 method does not comprehensively consider dependencies. To motivate this issue, consider the damage data and fragility function shown in Figure 1. The fragility function, represented by the solid line, specifies the probability that a gypsum wallboard partition experiences light cracking, as a function of the story drift ratio it experiences. The experimental data in the figure, as well as the resulting fragility function that was fit to these data, indicate that a partition wall may experience minor damage at drift ratios as low as 0.1%, but even at drift levels above 0.4% damage is not certain.

There are a number of potential causes for this observed variability in the demand levels that trigger component damage (e.g., FEMA, 2018, Section 3.8.1): 1) Damage is predicted by a scalar demand metric (e.g., story drift ratio), but actual damage is caused by a complex sequence of displacements, accelerations, and velocities during shaking. The demand metric is thus an imperfect representation of the loading on the component. 2) Components of the same 'type' have varying characteristics due to inherent randomness in the materials they are made of. 3) A particular contractor or subcontractor may do better or worse than typical when installing the component (e.g., in anchoring pipes and suspended ceilings). 4) A component fragility function represents a range of specific components and a range of construction means and methods, but a particular building will use a specific component (e.g., the 'glass curtain wall' component types in FEMA P-58 represent general categories of components rather than one specific model and installation detail).

The above sources of variability will influence multiple components throughout a building, rather than affecting each component independently. For example, for a given component type, the construction quality and specific component type will likely be similar throughout a building, leading the components to be damaged at a similar level of
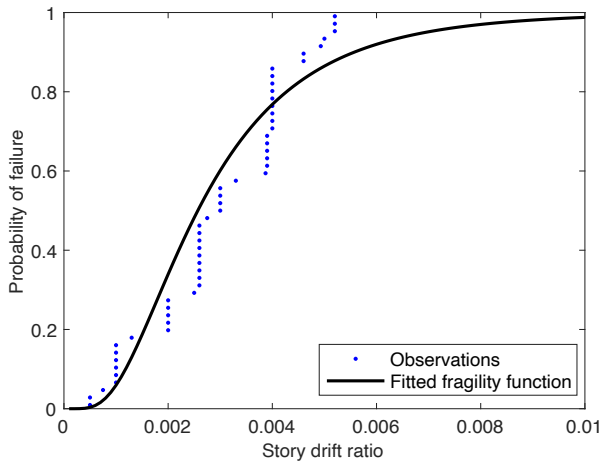
Figure 1. Experimental data and fragility function for gypsum wallboard partitions experiencing Damage State 1: first visible damage, light cracking. Points indicate the fraction of experimental components with observed damage at a given drift ratio, and the line indicates the fragility function that was fit to these data. Data are from Miranda and Mosqueda (2011).

demand. These can be accounted for by defining damage state dependencies. However, the prior FEMA P-58 method generally considers damage occurrence given EDP to be independent from component to component (with a limited exception for a few types of components that are assumed to all take the same damage state when co-located).

Further, some building loss metrics are sensitive to assumptions about damage state dependencies. To illustrate, consider an idealized building with 100 components, each of which would cause building closure if damaged, and each having a 0.01 probability of being damaged. If the components' damage occurrences are perfectly dependent (i.e., either all of the components are damaged, or none are), then the building has a 0.01 probability of closure. But if the components' damage occurrences are independent, then the building has a 0.63 probability of closure (each of the components has a 0.99 probability of functioning, so there is a $0.99^{100} = 0.37$ probability that no components are damaged and the building remains open). This difference in results indicates the potential importance of damage state dependencies in the assessment. Real buildings are more complex than this simple illustration, as component damage depends upon EDPs that vary throughout the building, and damage occurrences are neither perfectly dependent or independent. Those more realistic cases will be discussed below.

This paper proposes a general model to consider dependencies in component damage that has the following characteristics: 1) It is compatible with the Monte Carlo simulation approach for propagating uncertainties utilized by FEMA P-58. 2) It allows for dependencies in damage among components of the same type located throughout a building (e.g., identical ceiling tiles at multiple locations in the building), and

dependencies in damage amongst component types with similarities (e.g., concrete components that are all constructed by the same subcontractor). 3) Is simple to conceptualize and parameterize, so the degree of dependency can be estimated via judgment and easily documented.

These damage dependencies have been previously discussed in other risk analysis studies considering multiple components. Nuclear power plant risk assessment documents have noted the effect of component damage correlation on system failure probabilities since the 1980s (Smith et al., 1981). There have been multiple proposals for ways to address this. Reed et al. (1985) proposed bounding estimated system performance, but this approach has limitations (Segarra et al., 2021) and is not amenable to Monte Carlo analysis of the type used in FEMA P-58. Baker (2008) discussed Monte Carlo simulation of partially correlated component capacities, but only as a basic concept that did not consider multiple component types and multiple damage states. Segarra et al. (2021) proposed a Bayesian Network formulation that is more general, but is not compatible with the FEMA P-58 Monte Carlo simulation algorithm. Anup et al. (2022) recently proposed a parameterization of component fragilities similar to that proposed here, but with a focus on analytical system reliability calculations rather than Monte Carlo loss assessments, and without exploring numerical implementation or presenting system-level results to explore the impact of correlations.

Correlation of multiple spatially distributed components is also important to risk analysis of systems such as a portfolio of properties or a lifeline system with components located throughout a region (e.g., Bazzurro and Luco, 2004; Sousa et al., 2018). Several researchers have studied the importance of correlations in this context. Shome et al. (2012) proposed a model for spatial correlation of loss ratios that has the rare advantage of being empirically calibrated, but it is relevant for continuous-valued loss ratios rather than discrete damage states, and it was only calibrated for losses to wood houses. Lee and Kiremidjian (2007) and Heresi and Miranda (2022) proposed applying correlation to the discrete outcomes for each component, but their approaches are somewhat unwieldy to calibrate and implement, and are not designed for use in Monte Carlo simulations. The proposal presented here thus builds upon some concepts in the aforementioned prior literature, presenting a model that is straightforward to implement for multiple component types and damage states, and compatible with the Monte Carlo assessment approach utilized in the FEMA P-58 methodology.

The remainder of the paper first describes the prior FEMA P-58 component damage methodology. The proposed model with partial damage dependencies is then described and contrasted with the prior model. An idealized simple example is then presented, to build intuition regarding the impact of these dependencies. Finally, results from a realistic building analysis are presented, to quantify the practical impact of these dependencies, and to assess the sensitivity of the results to alternative parameter values for correlations.

Prior FEMA P-58 method

Here, we describe the prior FEMA P-58 method for simulating component damage, in order to highlight the adjustment made in the proposed method. This section also defines

relevant model parameters and documents the prior method so that it can later be used to produce example results.

The FEMA P-58 methodology uses a fragility function to estimate the probability of component damage from an EDP, p^*. The fragility function is defined as (Kennedy and Ravindra, 1984)

$$p^* = P(DS \geq ds_i | D = d) = \Phi \left(\frac{\ln d - \ln \theta_i}{\beta_i} \right) \tag{1}$$

where DS denotes the damage state of a given component, ds_i denotes the ith damage state threshold for that component (and damage states of increasing severity are associated with a larger value for the index i), D denotes the engineering demand parameter associated with the component's damage (e.g., story drift ratio), and d denotes the specific demand level from a Monte Carlo simulation of structural response. Here and throughout the manuscript, we denote random variables with uppercase letters, and numerical values with lowercase letters. On the right-hand-side of the equation, $\Phi()$ denotes the standard normal cumulative distribution function (CDF), and θ_i and β_i are parameters defining the shape of the fragility function for the given component and damage state. Specifically, θ_i is the demand level at which there is a 0.5 probability of component damage (the median), and β_i is the log-standard-deviation (or "dispersion").

Once the probability p^* is computed using Equation 1 with the appropriate fragility and demand parameters, Monte Carlo realizations of damage state outcomes are simulated. The component is simulated to be damaged with probability p^* or undamaged with probability $1 - p^*$ (FEMA, 2018, Volume 1, Section 7.5.1). When there are multiple components in the building, a separate p^* is computed for each component, and an independent damage simulation is generated for each component (FEMA, 2018, Volume 1, Section 7.5). This procedure is illustrated in Figure 2a.

Proposed method

Here we describe the proposed method for sampling of component damage, first for a single component, and then for multiple components.

Capacity sampling for a single component

The proposed approach treats the capacity of the component to withstand damage as the random variable to be sampled. This is in contrast to the prior method, where the binary outcome of damage or no-damage is the sampled random variable.

The capacity of the component is defined as:

$$\ln C_i = ln\theta_i + \beta_i \, \epsilon \tag{2}$$

where C_i is the capacity of the component to resist the ith damage state, in units of the EDP demand metric. If the demand on the component exceeds its capacity, the component will be damaged, and otherwise it will not. The parameters θ_i and β_i are the same as in Equation 1. Finally, ϵ is a standard normal random variable (i.e., with
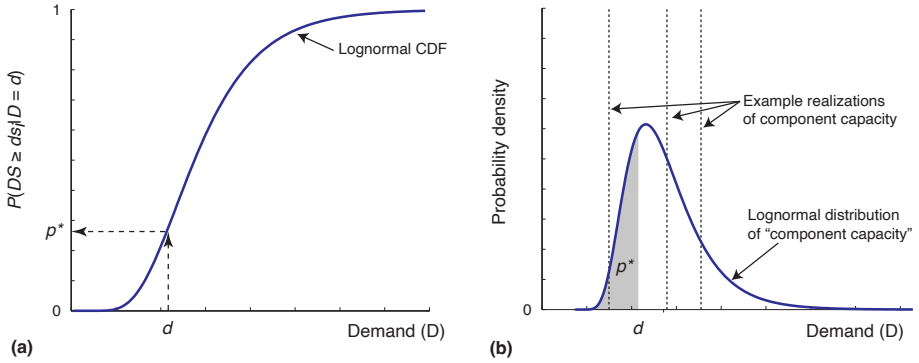
Figure 2. (a) Traditional method for sampling damage states for a given level of seismic demand, d. The fragility function is evaluated to compute the probability of damage (p^*). Then damage is sampled with probability p^* and non-damage with probability $1 - p^*$. (b) Proposed method of sampling damage states for a given level of seismic demand, d. A component capacity value is sampled from the Equation 2 capacity distribution. Example samples are indicated by the dashed step functions in the figure. The component is deemed damaged if the capacity is less than d. The capacity distribution is indicated by the superimposed distribution, and p^* of the capacity samples from that distribution (indicated by the shaded area) will be less than d.

mean of zero and standard deviation of 1). The random variable ϵ is the source of variability in component capacities and resulting damage outcomes, and the magnitude of this variability is controlled by the parameter β_i. The normally distributed ϵ is the sole source of uncertainty on the right-hand side, so $\ln C_i$ is normally distributed and thus C_i is lognormally distributed.

With this formulation, damage is simulated by generating a Monte Carlo simulation of ϵ, substituting it into Equation 2 to simulate a capacity value, and then comparing that capacity to the relevant demand value from a given simulation. This process is illustrated in Figure 2b. This process will produce identical results to the prior method, in terms of the fraction of damaged components that are simulated for a given value of demand, and given values of θ_i and β_i.

When a component has multiple damage states (and multiple associated θ_i and β_i) values, the damage state can be sampled by sampling a single ϵ value, pairing it with each θ_i and β_i value to get a C_i for that damage state, and assigning the component the highest damage state for which the demand exceeds C_i. Using a single ϵ value for all of the damage states will ensure that the fraction of samples having any specific damage state will equal the probability specified by the fragility functions. That is

$$\frac{n_{ds_i}}{n_{sims}} = P(DS \geq ds_i | D = d) - P(DS \geq ds_{i+1} | D = d) \tag{3}$$

where n_{ds_i} is the number of simulations of damage state i, n_{sims} is the total number of simulations, and the right-hand-side terms are the fragility function probabilities from Equation 1. Note that this use of a single ϵ value implies that a component's capacities across damage states are perfectly correlated.

Capacity sampling for multiple components

When considering multiple components, it is now straightforward to introduce dependence in their damage outcomes via the parameter ϵ in Equation 2. Sampling an independent ϵ value for each component produces independent damage outcomes, given the demand, the same as in the prior method. But sampling dependent ϵ values across components will produce dependence in the damage outcomes.

To introduce partial dependence in damage outcomes, and to facilitate the parameterization of dependence, we decompose the ϵ term of Equation 2, to represent this variability as a sum of contributions from multiple sources.

$$\ln C = \ln \theta_i + \beta_{all}\epsilon_{all} + \beta_{sys}\epsilon_{sys} + \beta_j\epsilon_j \tag{4}$$

where $\beta_{[\cdot]}$ is the dispersion, and $\epsilon_{[\cdot]}$ is a standard normal random variable, associated with each source of uncertainty. This decomposition into multiple ϵ terms allows these individual terms to be simulated in the Monte Carlo analysis, and re-used between some components, introducing correlation into those components' capacities.

We propose the following groupings of component capacity sources, in order of increasing specificity:

- all - common to all components in the entire performance model
- sys - common to all components from a given 'system' in the building
- j - specific to the jth individual unit of a component type

The 'all' and 'system' groupings are motivated by the sources of component damage correlation discussed in the Introduction. Example groupings of components into systems are provided in Table 1. These groupings follow the system groupings used in the Cook et al. (2022) methodology for functional recovery, and disaggregate structural components by trade. These approximately represent groups of components likely to be built by the same subcontractor.

When simulating damage to multiple components, some terms contributing to capacity variability will be shared among components. To illustrate, consider two components in the building which fall into the same system category (Figure 3). When the capacities of these components are simulated, a single realization of ϵ_{all} will be shared by both components, as well as all other components in the building (Figure 3a) and a single realization of ϵ_{sys} will also be used for both, and for all other components in that system type. Separate ϵ_j terms would be simulated for each component (Figure 3b). The shared ϵ terms will introduce correlation in the components capacities, as illustrated in the following equation and in Figure 3c.

Table 1. Sample component groupings for (a) structural and (b) non-structural components. Components within the same system all share a single ϵ_{sys} realization for a given Monte Carlo sample. The constituent component types column indicates the types of components in each system group.

(a)

System	Constituent component types
Concrete	Gravity System
	Link Beams
	Moment Connections
	Shear Walls
Steel	Base Plates
	Braces
	Gravity System
	Moment Connections
	Column Splices
Roof	Flexible Diaphragm
	Out-of-plane Connections
Masonry	Shear Walls
Cold Formed Steel	Shear Walls
Wood Light Frame	Cripple Walls
	Shear Walls

(b)

System	Constituent component types
Contents	General
	Medical
	Racks
Electrical	Batteries
	Distribution System
	Generators
	Motor Control Center
	Switchgear
	Transformers
Conveying	Elevators
Envelope	Cold Formed Steel
	Cladding
	Glazing
	Masonry Infill
	Wood Light Frame
Fire Suppression	Drops
	Piping
HVAC	Air Handling Units
	Air Distribution System
	Chilled Piping
	Chillers
	Compressors
	Control Panels
	Cooling Towers
	Steam Piping
Interior	Ceilings
	Floors
	Lighting
	Partition Walls
Plumbing	Potable Water
	Sanitary Waste
Roof	Chimneys
	Coverings
	Parapets
Stairs	Stairs

$$\ln C_1 = \ln \theta + \beta_{all}\epsilon_{all} + \beta_{sys}\epsilon_{sys} + \beta_j\epsilon_1$$

$$\textcolor{blue}{shared} \qquad \textcolor{red}{independent} \tag{5}$$

$$\ln C_2 = \ln \theta + \beta_{all}\epsilon_{all} + \beta_{sys}\epsilon_{sys} + \beta_j\epsilon_2$$

where C_1 and C_2 denote the two components' capacities, and ϵ_1 and ϵ_2 denote their component-specific contributions to capacity. The θ and β values will also in general vary by component, but subscripts on those terms are omitted above to highlight the model aspects that are most relevant to correlations.
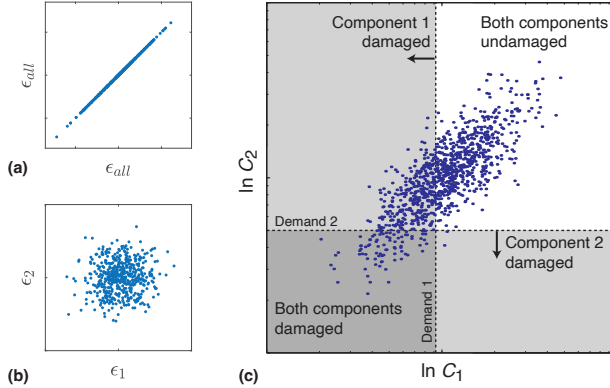
Figure 3. Monte Carlo simulations of residual terms and component capacities for two components. (a) Simulations of the ϵ_{all} term, of which a single value is used for both components in a given simulation. (b) Simulations of the ϵ_i term, which is independent for each component. (c) Simulations of the component capacities using Equation 4, along with illustrative damage thresholds. Points indicate component capacity simulations produced using Equation 5. The shaded regions indicate the capacity values for which capacity $<$ demand, and thus produce a damage outcome. Because the capacities of the components are partially correlated, the damage outcomes for the components are dependent.

The approach of decomposing the ϵ uncertainty term in Equation 2 into multiple contributions, with some being shared, is termed an equi-correlated model by Ditlevsen (1981). We also note that 'dependence' is a general term to describe probabilistic relationships in outcomes of component damage, while 'correlation' is a more narrow measure of linear dependence. Because the above log-capacity values have a multivariate normal distribution, dependence is fully described by the correlation in capacity values, so we can use 'correlation' and 'dependence' interchangeably in this context.

Parameterization

This section utilizes the model from the previous section, and reframes the equations into a format that is easy to implement and facilitates intuitive parameterization of correlations. The variance of $\ln C$ in Equation 4 is equal to

$$Var[\ln C] = \beta_{all}^2 + \beta_{sys}^2 + \beta_j^2 \qquad (6)$$

This variance should equal β^2 from Equation 1, for consistency with the component's original fragility function. It thus follows that the uncertainty can be partitioned to

individual sources while maintaining the overall capacity uncertainty, β, by satisfying the constraint

$$\frac{\beta_{all}^2}{\beta^2} + \frac{\beta_{sys}^2}{\beta^2} + \frac{\beta_j^2}{\beta^2} = 1 \tag{7}$$

The relative contributions of each uncertainty group can thus be quantified by relative 'weights', w, that sum to 1 and satisfy:

$$[w_{all}, w_{sys}, w_j] = \left[\frac{\beta_{all}^2}{\beta^2}, \frac{\beta_{sys}^2}{\beta^2}, \frac{\beta_j^2}{\beta^2} \right] \tag{8}$$

Substituting Equation 8 into Equation 4 to specify the capacity C in terms of weights, w, gives:

$$\ln C = \ln \theta + \beta \left[\sqrt{w_{all}} \epsilon_{all} + \sqrt{w_{sys}} \epsilon_{sys} + \sqrt{w_j} \epsilon_j \right] \tag{9}$$

The relative weights therefore determine how correlated the component capacities are with capacities of components of other types.

Fully *independent* component capacities would be achieved by placing weight only on the ϵ_j terms that are independently simulated for each component:

$$[w_{all}, w_{sys}, w_j] = [0, 0, 1] \tag{10}$$

Fully *dependent* component capacities would be achieved by placing weight only on the ϵ_{all} term that is shared amongst all components:

$$[w_{all}, w_{sys}, w_j] = [1, 0, 0] \tag{11}$$

Even with the fully dependent capacity model, the damage states could still differ amongst components with differing demands, but this model would produce much more similarity in damage states than that of Equation 10. Partially dependent component capacities can be produced by other combinations of weights.

Proposed model weights We propose using the following weights for the purpose of FEMA P-58 assessments:

$$[w_{all}, w_{sys}, w_j] = [0.2, 0.6, 0.2] \tag{12}$$

This model assumes that some of the uncertainty is shared by all components (20%), and some is shared by all components of the same system (60%), with the remainder unique to each component. Equation (12) is motivated by the observation that most sources of component damage variability that were described in the Introduction will vary by system (e.g., subcontractor construction quality and the specific component in a building relative to a broader set of components of that type), suggesting that the largest weight should be on ϵ_{sys}. Some sources of variability may be relatively common throughout the building (e.g., the time series of displacements, velocities, and accelerations experienced in a given earthquake, and the overall quality of construction) and some sources of variability

are likely to be inherent to a single component, suggesting that some weight should also be placed on the ϵ_{all} and ϵ_j terms as well.

Example results presented below suggest that some building performance metrics are strongly affected by the choice of fully independent, fully dependent, or partially dependent component damage. However, for a partially dependent component damage model such as Equation 12, modest changes to the relative weights have much lesser impact (see the Supplemental Materials for results to support this statement). The proposed model is thus believed to capture the important characteristic of partially dependent damage, without being highly dependent on the specific choice of weights.

Model generalizations Equation 4 was presented to be compatible with the proposed model weighting. But the equations and model weights can be generalized in several ways if desired, while still maintaining the general characteristic of partial correlations.

First, the number of ϵ terms in Equation 4 can be varied. For example, additional terms could be included in the formulation that are shared only amongst components of a single constituent component type, as listed in Table 1. Also, an ϵ term could be included that is shared amongst components of a single Performance Group (in FEMA P-58 parlance, these are components of the same type that are affected by the same EDP). If an ϵ term is included based on performance groups, and all the weight applied to that term, then this approach would reproduce the 'correlated fragility' option that is noted in the prior FEMA P-58 methodology (FEMA, 2018, Volume 2, Section 2.4.6). Additional terms are simple to add algorithmically: all that is required is a mapping to indicate which components in the building share each ϵ term. But additional terms require additional weights and component groupings, and this additional complexity was not deemed justified in this case, given the lack of empirical data to constrain the weight values.

Second, the weight vector of Equation 8 does not need to be fixed for all components in the building. Components of different types can have unique weight vectors. This might be appropriate if one believed, for example, that concrete components and mechanical components had differing within-system correlations in their capacities. This is straightforward from an algorithmic perspective, and numerically valid. Nevertheless, the lack of empirical data to constrain these models led to a preference for the simpler proposed model at present.

Third, dependence in component capacities does not need to be specified via the above decomposition of ϵ into multiple contributing sources. Instead, dependence could be introduced by sampling capacity terms for each component from a multivariate distribution and specifying a covariance matrix for that distribution. It can be shown that the above decomposition weights can be converted into equivalent covariance values. However, the authors and project reviewers found the above weighting approach more intuitive for specifying judgment-based dependencies.

Simple example

To illustrate the impact of this formulation, we first present results for a highly idealized case. We consider a four-story building, with story drift ratio (SDR) as the EDP of interest. The EDPs would usually be estimated from structural analyses. But, for illustration here, we assume they are lognormally distributed with a median of $\theta = 0.02$, a log-standard deviation of $\beta = 0.5$, and correlations between stories of $\rho_{\ln SDR_i, \ln SDR_j} = 0.6$ (where ρ denotes a correlation coefficient, and SDR_i and SDR_j denote SDR on stories i and j, respectively). Each story has one each of five types of components, each type from a unique system. Each component has a single damage state, with fragility parameters $\theta = 0.05$ (in units of story drift ratio) and $\beta = 0.5$. In other words, the median drift demand on each story is 2%, the median drift capacity is 5%, and the variability in demands and capacities is such that the probability of any single component failing is approximately 0.1.

Figure 4 shows component damage statistics for three permutations of analyses. In all three cases, the model parameters in the above paragraph are used. The only difference among the three cases are the assumed component correlations. We use the $[w_{all}, w_{sys}, w_j]$ characterization of Equation 9, and consider three sets of numerical values for the weights.

Figures 4a and 4b show results for $[w_{all}, w_{sys}, w_j] = [0, 0, 1]$. Each of the 20 components in the building has an independent capacity, since all weight is on the ϵ_j term that is unique for each component. Figure 4a shows the histogram of the number of damaged components in each simulation, from 10,000 total Monte Carlo simulations. It shows that 60% of the simulations produce at least one damaged component, but only 2.4% produce 10 or more damaged components. Figure 4b shows a scatter plot of how many components of "type 1" and "type 2" are damaged in each simulation (where the numbering is used to distinguish between types, but otherwise has no meaning as all five component types have the same fragility parameters). Each component type could have between 0 and 5 components damaged, and the plotted points are jittered by a small amount so that the number of repeated outcomes can be seen. This figure shows that there is little correlation between the number of damaged components of each type, as would be expected because their capacities are independent (although there is some correlation because the components on a given floor are all subjected to the same demand value). This case is equivalent to the prior FEMA P-58 assessment approach, with the small exception of some component types that are correlated by performance group.

Figures 4c and 4d show results for $[w_{all}, w_{sys}, w_j] = [0.5, 0, 0.5]$. This case produces partial correlations in component capacities, for components of all types and on all floors, since all 20 components in the building share the ϵ_{all} variable that now gets 0.5 weight. The effect of this partial correlation can be seen in Figure 4c where now only 44% of simulations produce a damaged component (versus 60% in the Figure 4a), because some simulations have a large ϵ_{all} value and cause all 20 components to have a higher capacity and be more likely to avoid damage. Because of this partially correlated capacity, the number of simulations with ≥ 10 damaged components increases to 5.6%. The partially correlated capacities also result in the number of damaged components of a given type

being more correlated in Figure 4d (as evidenced by the greater number of points lying close to the diagonal on the figure).

Finally, Figures 4e and 4f show results for $[w_{all}, w_{sys}, w_j] = [1, 0, 0]$. In this case, all 20 components in the building will have identical capacities for a given simulation, because only the shared ϵ_{all} variable is contributing to capacity variation. Figure 4e shows a much different pattern of damage, with only 19% of simulations producing damage, but 11% producing 10 or more damaged components. This is because the 20 components all have identical capacities in this case, per Equation 9, so they tend to all be undamaged, or all be damaged (with the only the story-to-story variation in SDR demands producing some differing damage state outcomes throughout the building). There is still some variation in demand across the building's stories, so components on differing stories can still take differing damage states. But on a given story, the five components all have the same demand and capacity and so will take the same damage state. This is seen in Figure 4e, where the numbers of damaged components are only multiples of five, and in Figure 4f, where the number of damaged components are perfectly correlated between the two types.

These cases provide an indication of how component capacity correlation affects building-level damage features. In all three cases, the mean number of damaged components, $\overline{N}$, is *unchanged*. The left panels indicate that the average number is two, as expected, since there are 20 components, each with a 0.1 probability of damage. So, average metrics such as mean repair cost are, to a first order, not impacted by these correlations. However, the probability of non-zero damage *decreases* with increasing component correlation, as indicated by the $P(N \geq 1)$ metrics in the left panels. If, hypothetically, this building would be red-tagged if any component were damaged, then the uncorrelated (Figure 4a) case would have the highest probability of triggering a red tag. Conversely, the probability of extreme damage *increases* with increasing component correlation, as seen in the $P(N \geq 10)$ metrics in the left panels. This pattern would influence higher-percentile loss predictions such as "probable maximum loss" analyses that predict 90th-percentile impacts for a given loading intensity.

This simple example is intended to build intuition about the role of component capacity correlations on predicted building-level impacts, and to demonstrate that the impact of correlations depends upon the building-level metric of interest.
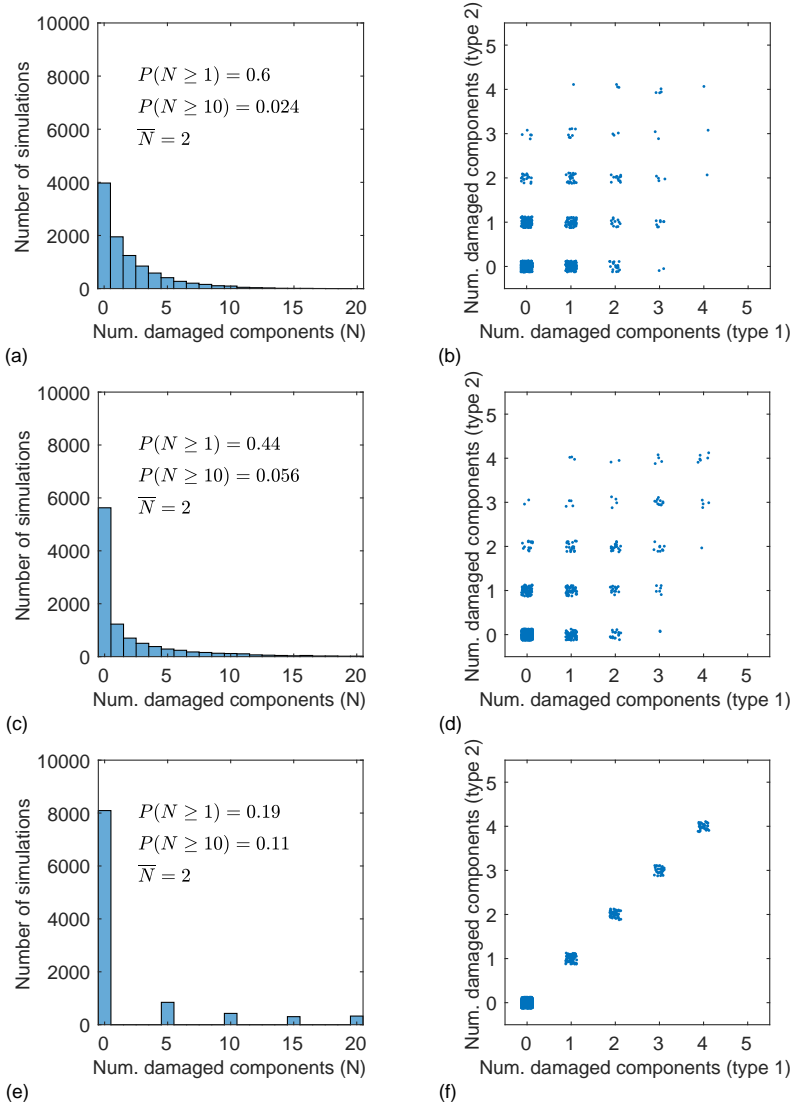
Figure 4. Component damage statistics for the simple example, under varying component damage correlation models. (a, b) no correlation, $[w_{all}, w_{sys}, w_j] = [0, 0, 1]$. (c, d) partial correlation: $[w_{all}, w_{sys}, w_j] = [0.5, 0, 0.5]$. (e, f) full correlation: $[w_{all}, w_{sys}, w_j] = [1, 0, 0]$. The left-hand panels report statistics for the probability of a simulation producing at least one damaged component ($P(N \geq 1)$), the probability of a simulation producing at least ten damaged components ($P(N \geq 10)$), and the mean number of damaged components ($\overline{N}$).

Realistic example

To illustrate the impact of these component correlations in more complex and realistic cases, we present results for several performance metrics of a case study building. We consider a 20-story steel moment frame office building located in Los Angeles, California, following ASCE 7-16 seismic design requirements (ASCE, 2016). Ground motion hazard is computed using U.S. Geological Survey (2014) probabilistic hazard results. The quantities and types of damageable components in the building are based on the office occupancy, and on building code requirements, as embedded in the FEMA P-58 normative quantities. Joint probability distributions of drifts and accelerations at all floors, for a range of IM levels, are predicted using a statistical model calibrated statistically based on response history analyses of similar buildings (Cook et al., 2018). Component damage states and repair costs are predicted using FEMA P-58 fragility functions (FEMA, 2018), and red-tagging and recovery metrics are computed using the methodology of Cook et al. (2022). The red tagging approach looks at groups of structural components, and damage states to those components that are severe enough to cause loss of lateral or gravity load carrying capacity. If the number of damaged components in these damaged states exceed a threshold, then the building is "red tagged" (Cook et al., 2021). The analyses were performed using the SP3-RiskModel software.

Table 2 describes several $[w_{all}, w_{sys}, w_j]$ weighting schemes that are considered to provide intuition as to how sensitive building performance metrics are to different weighting choices. Figures 5-7 show the differences in building performance metrics resulting from various weights.

Figure 5 shows the sensitivity of red tagging results to various correlation models. In this and the following figures, damage simulations are run conditional on uniform hazard spectra at varying amplitudes. The horizontal axis of Figure 5a plots Peak Ground Acceleration as the intensity measure, for ease of interpretation, though any other spectral ordinate from the uniform hazard spectra could be used instead.

Figure 5 shows that, as expected, the 'Prior P-58' and 'Component' schemes are identical (because there are no components categorized as "correlated" using the prior P-58 scheme). These fully uncorrelated cases are the upper bound for red tag probability because the lack of correlation results in more cases where just a few components are damaged, but this still triggers a red-tag, as discussed in the Simple Example Section. Conversely, the other extreme is the fully correlated case, 'All,' which sees more zero-damage realizations and therefore predicts the lowest red-tag probabilities. The 'System' scheme produces equivalent red tag results to the 'All' scheme because the structural system components remain fully correlated, and the other component types do not affect the red tagging outcome. Between these two extremes are the 'Even' and 'Recommended' cases, which each put partial weights all of the three weight categories. As discussed in the Proposed Model Section, there is insufficient empirical data to precisely calibrate these weights, but the reasonable agreement between the 'Even' and 'Recommended' cases (less than 0.05 difference in probability) indicates the low sensitivity of results to the specific weights considered.

Table 2. Summary of weighting schemes used to produce building-level performance metrics for the realistic example building.

Scheme name	$[w_{all}, w_{sys}, w_j]$	Notes
Recommended	$[0.2, 0.6, 0.2]$	The recommended weighting scheme, as discussed in the Proposed Model Section.
Even	$[1/3, 1/3, 1/3]$	Even weights are applied to each category, to simulate some capacity correlation between and within systems.
All	$[1, 0, 0]$	The capacity of all components in the building are fully correlated.
System	$[0, 1, 0]$	The capacity of components in the same system are fully correlated, but there is no correlation between systems.
Component	$[0, 0, 1]$	The capacity is not correlated between or within systems. (This is equivalent to the 'Prior P-58' scheme when no correlated components are included in the model.)
Prior P-58	N/A	This is the prior FEMA P-58 correlation model, where most components are independent, and a few components are perfectly correlated within a performance group.
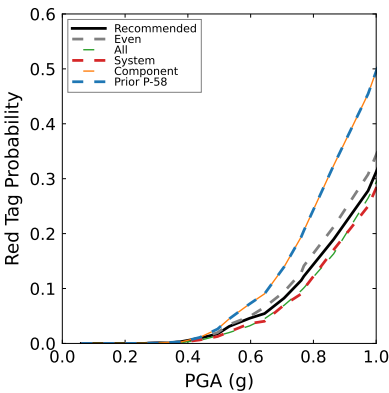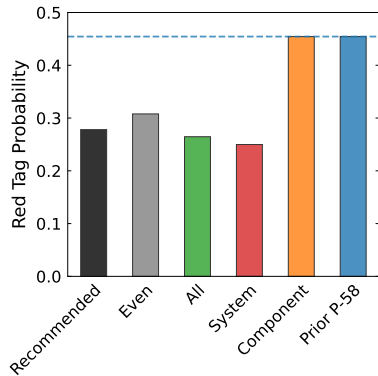
(a)   **(b)**

Figure 5. Red tagging metrics for the 20-story steel perimeter moment frame building for various $[w_{all}, w_{sys}, w_j]$ weighting schemes. (a) Red tag probabilities as a function of the PGA value associated with each uniform hazard spectrum. (b) A 'vertical slice' of results from (a) at $PGA = 0.95$ g, which has a return period of 2475 years at the building location.

Figure 6 shows the case study building's mean, median, and 90th percentile loss ratios (i.e., the repair costs divided by the building's replacement value). The Simple Example section demonstrated that the correlation does not affect the mean number of damaged components. Figure 6a confirms this by showing that the mean loss ratio is unaffected by the correlation model (any slight apparent variations result from the randomness of the Monte Carlo simulations). In detailed loss simulations such as these, it is possible that non-linearity in repair costs due to volume discounting (lower per-unit costs for higher quantity repairs) could produce some difference in mean costs for high-damage cases, though that effect is inconsequential for this case.

Figures 6b and 6c show the median and 90th percentile losses, respectively. The two metrics have opposite trends; the 90th percentile loss increases, and the median loss decreases, for the cases having stronger correlation. Both of these effects are due to the increased likelihood of extreme outcomes (i.e., very many or very few components simultaneously being damaged). Figure 6d summarizes these opposing trends for the analyses performed at the 2475-year ground motion level ($PGA = 0.95$g).

Figure 7 shows the effect of correlation models on reoccupancy and functional recovery time calculated using the methodology of Cook et al. (2022). With this methodology, to maintain occupancy, most structural components should be in low-to-moderate damage states such that the building is not tagged as unsafe; cladding, ceilings and equipment should not pose falling hazards; and stairs should maintain vertical load carrying capacity to support building egress. For building function, critical MEP equipment and distributed components, such as air handling units, potable and sanitary piping, and electrical switchgear, should continue to operate to support basic tenant function. The plots show the probability that the building is not reoccupiable at 30 days (Figures 7a and 7b) and not functional (Figures 7c and 7d) 30 days after shaking of the given intensity occurs. The plots demonstrate that the 'Prior P-58' and 'Component' weighting schemes result in the highest probability of failure of the functional recovery measures due to the lack of correlation, which produces the lowest amount of 'no damage' (or acceptably low damage) realizations as discussed in the Simple Example Section. Conversely, the 'All' variant results in the lowest probability of failure because the correlation between all components is high and results in a larger number of 'no damage' (or acceptably low damage) realizations. Here acceptably low damage implies damage that does not trigger function or reoccupancy problems. In terms of component capacity, the high correlation ensures that the capacities are all relatively low or relatively high in the same realization, so there is less likely to be an outlying 'low' capacity component that prevents use of the building. Between these extremes are the the other variants 'System', 'Even', and 'Recommended'. The 'System' variant for reoccupancy is closer to the 'All' variant because there are fewer systems that matter for reoccupancy than function, so the correlations across systems have less impact on this metric.

The results of this case study demonstrate that a reasonable distribution of weights over the three sources of variability will produce a reasonable result bounded by the fully correlated and fully uncorrelated cases.
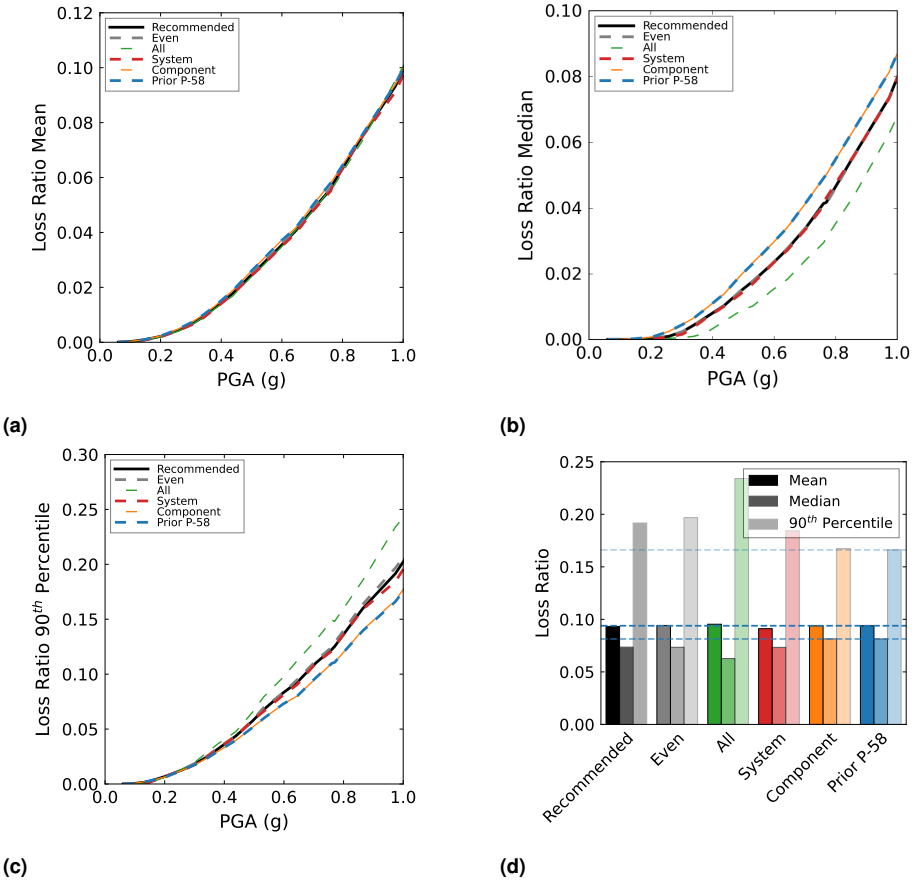
Figure 6. Loss metrics for the 20-story steel perimeter moment frame building for various $[w_{all}, w_{sys}, w_j]$ weighting schemes. (a) Mean loss ratio. (b) Median loss ratio. (c) 90th percentile loss ratio. (d) All loss ratio metrics, given shaking with $PGA = 0.95$g, which has a 2475-year return period. Note that the vertical axis limits on subfigures a-c are varied, to highlight trends within a given subfigure.

(a)

(b)

(c)

(d)
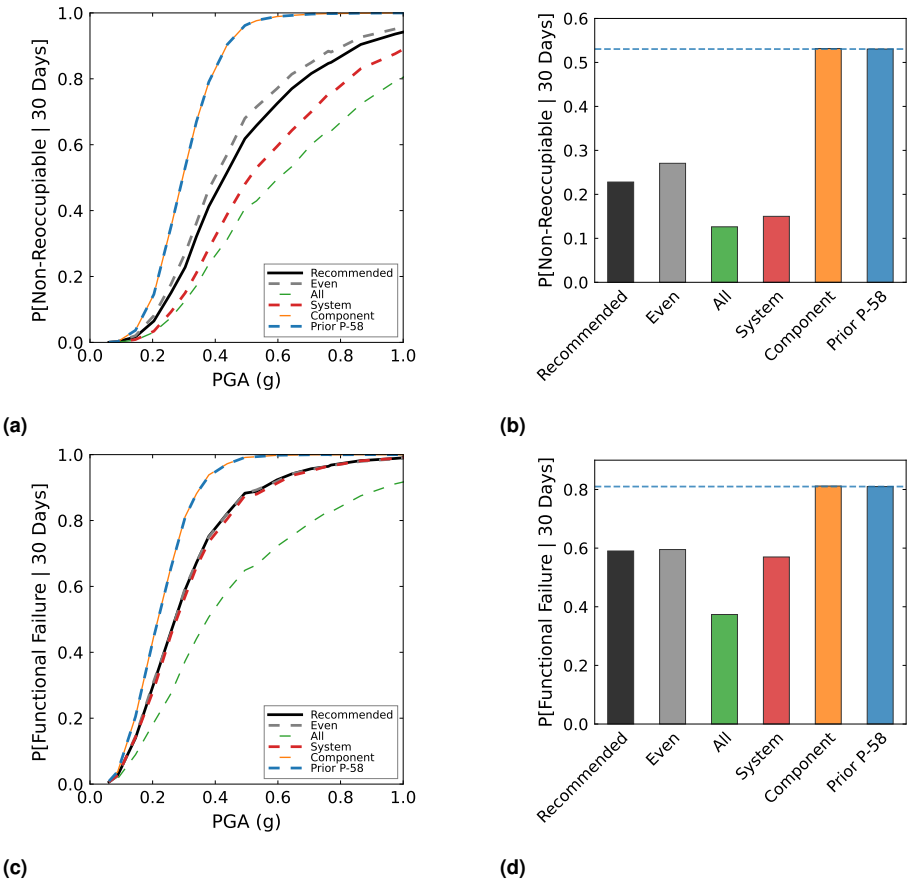
Figure 7. Functional recovery time metrics for the 20-story steel perimeter moment frame building, using the Cook et al. (2022) and various $[w_{all}, w_{sys}, w_j]$ weighting schemes. (a) Probability of loss of reoccupancy 30 days after shaking, for multiple ground motion amplitude levels. (b) Probability of loss of reoccupancy 30 days after shaking, given shaking with a 144-year return period ($PGA = 0.3$g). (c) Probability of loss of function 30 days after shaking. (d) Probability of loss of function 30 days after shaking, given shaking with a 144-year return period.

Conclusions

This paper proposes a practical method for incorporating partial dependencies in component damage outcomes when using Monte Carlo simulation to estimate risk to systems composed of multiple components. The method is flexible in allowing dependencies that vary based on location in the building, component type, and other factors. For individual components, the probabilities of damage obtained with this method are identical to prior approaches. For multiple components, this approach can reproduce traditional approaches if desired, but can be generalized to more plausible formulations that allow partial dependencies. Example results illustrate the impact of component capacity correlations on loss results.

The proposed method requires the specification of numerical correlation values. While direct empirical data to constrain dependencies remains elusive, the formulation does provide a conceptually appealing parameterization of the problem. That is, the analyst must specify how much of the variance in outcomes results from various sources (as opposed to specifying less-intuitive metrics of dependence). A parameterization for use in FEMA P-58 analysis is proposed that improves the realism of loss simulations relative to the prior approach.

While a parameterization has been proposed here based on current judgement, further study of damage data offers the opportunity to refine the parameterization. One data analysis approach that would be informative would be to perform component damage tests that hold some conditions fixed (e.g., construction method) and vary another (e.g., loading protocol), in order to quantify how much component capacity variability comes from each source of uncertainty. Another approach would be to use random effects models to study data sets like that in Figure 1 and attribute observed variability to the tests' varying component configurations, loading conditions, and other factors. From a modeling perspective, some components' damage could be studied by using high-fidelity numerical models (e.g., for steel connection fractures) and varying component and material characteristics, as well as loading time series.

The method was presented with a focus on the FEMA P-58 assessment methodology, but is relevant to other assessment situations that consider multiple components and fragility functions. Only the grouping of elements and correlation structure would need to be revisited to apply the method in other contexts focused on components with lognormal fragility functions, given the widespread use of this formulation. However, the method could be applied in other situations with other distribution types, as long as the capacity distribution for the component can be decomposed into shared and independent contributions to capacity.

Code and data availability

Demonstration code that implements the proposed model, and produces the results presented in the Simple Example section, is available at `https://github.com/bakerjw/FEMA_P58_damage_correlation`.

References

Anup A, Talaat MM, Grant FF and Ferrante F (2022) Quantifying Partial Fragility Correlations in Seismic Probabilistic Risk Assessments. In: *SMiRT-26*. Berlin/Potsdam, Germany.

ASCE (2016) *Minimum Design Loads for Buildings and Other Structures, ASCE 7-16*. ASCE/SEI 7-16. Reston, Virginia: American Society of Civil Engineers/Structural Engineering Institute.

Baker JW (2008) Introducing correlation among fragility functions for multiple components. In: *14th World Conference on Earthquake Engineering*. Beijing, China, p. 8.

Bazzurro P and Luco N (2004) Effects of Different Sources of Uncertainty and Correlation on Earthquake-Generated Losses. In: *1st International Forum on Engineering Decision Making (IFED)*. Stoos, Switzerland, p. 20.

Cook D, Wade K, Haselton CB, Baker JW and DeBock DJ (2018) A structural response prediction engine to support advanced seismic risk assessment. In: *Eleventh U.S. National Conference on Earthquake Engineering*. Los Angeles, California, USA.

Cook DT, Liel AB, DeBock DJ and Haselton CB (2021) Benchmarking FEMA P-58 repair costs and unsafe placards for the Northridge Earthquake: Implications for performance-based earthquake engineering. *International Journal of Disaster Risk Reduction* 56: 102117.

Cook DT, Liel AB, Haselton CB and Koliou M (2022) A framework for operationalizing the assessment of post-earthquake functional recovery of buildings. *Earthquake Spectra* 38(3): 1972–2007. DOI:10.1177/87552930221081538.

Cornell CA and Krawinkler H (2000) Progress and Challenges in Seismic Performance Assessment. *PEER Center News* 3(2).

Ditlevsen O (1981) *Uncertainty Modeling: With Applications to Multidimensional Civil Engineering Systems*. New York; London: McGraw-Hill International Book Co. ISBN 0-07-017046-0.

FEMA (2018) Seismic Performance Assessment of Buildings. Technical Report FEMA P-58, Prepared by Applied Technology Council for the Federal Emergency Management Agency.

Haselton CB, Hamburger RO and Baker JW (2018) Resilient Design and Risk Assessment using FEMA P-58 Analysis. *Structure Magazine* (March): 12–15.

Heresi P and Miranda E (2022) Structure-to-structure damage correlation for scenario-based regional seismic risk assessment. *Structural Safety* 95: 102155. DOI:10.1016/j.strusafe.2021.102155.

Kennedy R and Ravindra M (1984) Seismic Fragilities for Nuclear Power Plant Risk Studies. *Nuclear engineering and design: an international journal devoted to the thermal, mechanical and structural problems of nuclear energy* 79: 47–68.

Lee R and Kiremidjian AS (2007) Uncertainty and correlation for loss assessment of spatially distributed systems. *Earthquake Spectra* 23(4): 753–770.

Miranda E and Mosqueda G (2011) Seismic Fragility of Building Interior Cold-formed Steel Framed Gypsum Partition Walls. *Background Document FEMA P-58/BD-3.9* 2.

Moehle J and Deierlein GG (2004) A framework methodology for performance-based earthquake engineering. In: *Proceedings, 13th World Conference on Earthquake Engineering*. Vancouver, Canada.

Petersen MD, Moschetti MP, Powers PM, Mueller CS, Haller KM, Frankel AD, Zeng Y, Rezaeian S, Harmsen SC, Boyd OS, Field EH, Chen R, Rukstales KS, Luco N, Wheeler RL, Williams RA and Olsen AH (2014) Documentation for the 2014 Update of the United States National Seismic Hazard Maps. Technical Report Open-File Report 2014–1091, U.S. Geological Survey.

Porter KA, Kiremidjian A and LeGrue J (2001) Assembly-based vulnerability of buildings and its use in performance evaluation. *Earthquake Spectra* 17(2): 291–313.

Reed JW, Mc Cann Jr MW, Iihara J and Tamjed HH (1985) Analytical techniques for performing probabilistic seismic risk assessment of nuclear power plants. In: *International Conference on Structural Safety and Reliability (ICOSSAR 85)*. Kobe, Japan.

Segarra JD, Bensi M and Modarres M (2021) A Bayesian Network Approach for Modeling Dependent Seismic Failures in a Nuclear Power Plant Probabilistic Risk Assessment. *Reliability Engineering & System Safety* : 107678DOI:10.1016/j.ress.2021.107678.

Shome N, Jayaram N and Rahnama M (2012) Uncertainty and spatial correlation models for earthquake losses. In: *15th World Conference on Earthquake Engineering (WCEE), Lisbon*.

Smith PD, Dong RG, Bernreuter DL, Bohn MP, Chuang TY, Cummings GE, Johnson JJ, Mensing RW and Wells JE (1981) Seismic safety margins research program. Phase I final report-Overview. Technical Report NUREG /CR-2015, Prepared by Lawrence Livermore Laboratory for the U.S. Nuclear Regulatory Commission.

Sousa L, Silva V, Marques M and Crowley H (2018) On the treatment of uncertainty in seismic vulnerability and portfolio risk assessment. *Earthquake Engineering & Structural Dynamics* 47(1): 87–104. DOI:10.1002/eqe.2940.